Development of Electrical Impedance Spectroscopy and Tomography System

Ji-Jer Huang, Don-Ming Wu, and Chih-Hsuan Li

Department of Electrical Engineering, Southern Taiwan University, Tainan, TAIWAN

Abstract—Electrical impedance tomography (EIT) technology belongs to the functional imaging technologies. The EIT technique has several advantages, such as noninvasiveness, affordability, portability, and capabilities for high-speed monitoring and providing functional information. By contrast, electrical impedance spectroscopy (EIS) is a technology for obtaining bio-impedance measurements at different frequencies. This method has been used in many medical inspection studies. Hence, the purpose of this project was to set up a real-time EIT system. The system is modular, containing a digital sine waveform generator (with 0° and 90° phases), current generators with controller, a digital demodulator, an image reconstruction, and a simulation tank. Moreover, three image reconstruction algorithms were developed for the system software; including the weighted back-projection method and Newton's one-step estimated reconstruction algorithm. A high-speed DSP module (TMS320F28335) was utilized for obtaining voltage measurements by digital demodulation. The algorithms for the analysis and image reconstruction were implemented by another DSP module (TMS320C6713) to achieve the real-time goal. For the finished system, a correlation test indicated a highly linear relationship between the measured value and the actual value. Then, impedance values were measured at 0° or 90° and the cross-sectional image was reconstructed. When the separately placed copper target and Teflon target were tested, the cross sections of the electrical impedance tomography were obtained. In addition, the system is supported by a graphical user interface to extract and analyze the electrical impedance data as well as reconstruct the image.

Keywords: Electrical Impedance Tomography, Electrical Impedance Spectroscopy, Digital demodulation

1. Introduction

Electrical impedance tomography (EIT) is a technique for producing an image of the cross-sectional impedance within an object by applying currents while measuring the voltages at the boundary [1]. There are both the resistivity and permittivity distributions in the impedance image. In addition, EIT is different from the image modalities currently available in clinics, such as X-ray computed tomography, magnetic resonance imaging, emission computed tomography, and sonography. This technique can provide additional information on tissues under diagnosis. In comparison with computed tomography, EIT offers the merits of low cost, no radiation, and noninvasiveness. Several research groups have published reports about the EIT system [2,3]. Electrical impedance spectroscopy (EIS) is a scanning frequency measurement system that can provide more useful information about tissues and cells. Researchers conduct EIS studies in vivo for human tissues such as those of the bladder, skin, stomach, and breast. If electrical impedance were not used, there would be no choice but to perform a biopsy or use traditional imaging. Measurements from EIS and other technologies have been compared. The method is regarded as a better assessment tool than the traditional imaging method [4]. Some investigators even attempt to regard the method as a clinical diagnostic tool [4,5]. Other researchers have discussed how both the imaginary part and real part of the measured signal include some physiological and pathological information about the biological target. In this study, a combined EIS and EIT system is developed. The system utilizes the technology of direct digital synthesis (DDS) in the sine signal generator with phase-varying function. A voltage controlled current source with an enhance Howland circuit is used [6]. Two digital signal processors (DSPs) that possess high-speed computing capability are employed as kernels of demodulation and image reconstruction, respectively. This system supports two

simulation tanks; one is a miniature tank with a diameter of 1.5 cm, and the other is a normal tank with a diameter of 28.4 cm. At the same time, the system communicates with a PC via a USB interface and offers a friendly graphical user interface.

2. Materials and methods

2.1. System Architecture

As shown by its block diagram in figure 1, the overall system contains 32 independent channels for applying the currents to the object. The system hardware consists of five major parts: digital sine waveform generator, current generators with controller, digital demodulator, image reconstruction, and simulation tank. (I) Digital sine waveform generator: In this subsystem, the technology used is that of the direct digital synthesizer. The DDS chip (AD9851) manufactured by Analog Devices Co. produces the step-sine waveform. The AD9851 provides a program for phase modulation to enable phase shifting by 0° or 90°, while the signal frequency is variable from 100 Hz to 100 kHz. The signal is fed into a Butterworth low-pass filter with a cutoff frequency of 1 MHz. Finally, the smooth sinusoidal waveform is connected with the terminal of the DAC modulator through buffers. The signal is subsequently used as a reference in the demodulation. (II) Current generators and controller: The amplitude of the sinusoidal waveform, adjusted by the DAC and controlled by the MCU, was fed into the terminal of a voltage controlled current source (VCCS). The resolution of the DAC is 12 bits. The range of the current for each channel is within ±1 mA rms. The current source created in the VCCS with an enhanced Howland circuit is applied to the object through buffers with high input impedance and strong ability to drive current. (III) Digital demodulation: The voltage of each electrode is connected to the input of an instrument amplifier. Then, the amplified signal is fed into the analog to digital converter that has 12 bits of resolution and lies within the TMS320F28335 DSP chip manufactured by Texas Instruments Inc. The chip is a floating-point digital signal processor with a 32-bit CPU and Harvard bus architecture. The sampling rate for the system is greater than 1MHz. The algorithm of digital demodulation is implemented on-chip. (IV) Image reconstruction: The image reconstruction algorithms are implemented by the TMS320C6713 chip manufactured by Texas Instruments Inc. In addition, this chip is a floating-point digital signal processor with high-speed processing at the rate of 1.35 giga-floating-point operations per second. (V) Simulation tank: In order to test and validate the system performance, a simulation phantom was built. In this phantom, 32 electrodes made of copper and coated with gold were attached to the interior surface of a circular acrylic container. The diameters of the miniature and normal tanks were 1.5 and 30 cm, respectively. Their depths were 1.0 and 6.5 cm. The electrodes were 0.14 and 2.50 cm in width, as shown in figure 2. The circular container is filled to 60% of its depth with any of the different saline solutions having electrical conductivities over the range of interest. Targets with different geometries and conductivities are then placed in the bath. Metal or plastic targets are simulated as conductivities of infinity and zero. The personal computer is used as the kernel of the system to display and collect information.
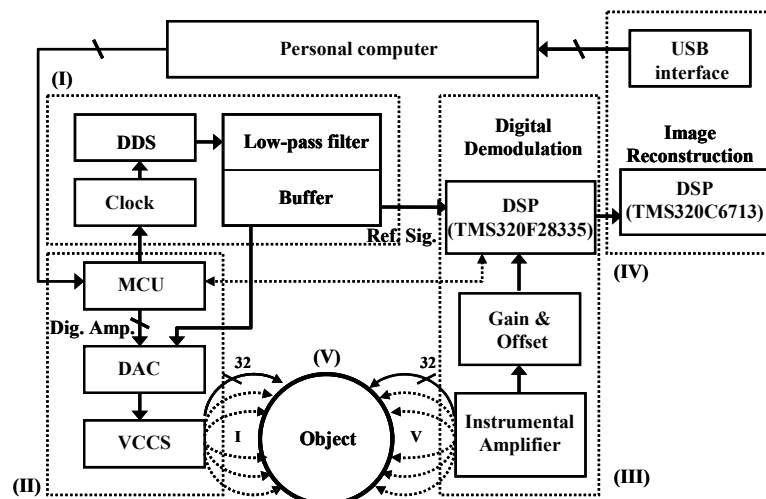

Fig. 1: Block diagram of system

2.2. Digital demodulation

The impedance measurement procedure applies a known current to the object with unknown impedance. The demodulation techniques are used to estimate the amplitude of the measured signal. In comparison with the traditional analog type of amplitude demodulation, the digital demodulation reduces the distortion of the signal by nonlinearity, DC drift, and noises. The processing can be realized inside the digital signal processor by multiplying the measured signal.

2.3. Reconstruction Algorithm

In general, there are two methods for solving the forward problem. One is the analytical method, and the other is the finite element method (FEM). The latter method is practical to represent the inhomogeneous or homogeneous media within the body. In addition, the purpose is to simplify the nonlinear governing equation into a system of linear algebraic equations. Hence, the finite element method is typically used in the iterative reconstruction algorithm. The aim of the reconstruction algorithm is to solve the inverse problem of the Laplace equation for the distribution of resistance within a region. Several techniques have been used to reconstruct the conductivity or resistivity distributions. In this project, the system utilizes three methods, including weighted back-projection and Newton one-step estimated reconstruction (NOSER). These are iteratively implemented as reconstruction algorithms by the system. By making a weighted back-projection reconstruction, the dynamical or relative image distribution is obtained, and the method supports a high frame rate for images. According to several research documents, however, the Newton-Raphson method has been found superior for obtaining the absolute image distribution. Thus, an algorithm based upon the Newton-Raphson method was used for image reconstruction. In fact, this iterative algorithm involves both forward and inverse algorithms. The NOSER method is employed to obtain the best initial estimate of the resistivity distribution inside the object. Then, the calculated distribution is mapped onto the mesh of the finite element method in order to acquire the resistivity of each element. The least-squares method is applied to monitor the differences between the boundary voltages from FEM computations and real measurements.

2.4. Software design

The system provides two functions, which are electrical impedance spectroscopy and electrical impedance tomography. Therefore, the system offers users a graphical user interface by which to manage its operation. Figure 2 shows the flowchart of the system program implemented using Visual C#. For this study, we took a left semicircle of a Cole-Cole plot from measurements at higher frequency. The k items of resistance (R) and reactance (X) were obtained for different frequencies. The least-squares method was employed to perform iterative fitting computations. The k items of the measurements were substituted into the iterative formula. The error function attained the convergence condition of $(r_n \cdot 0.0001)^2$. Approximations for x_0, y_0, and r were thus obtained and were subsequently used to derive the four characteristic parameters.
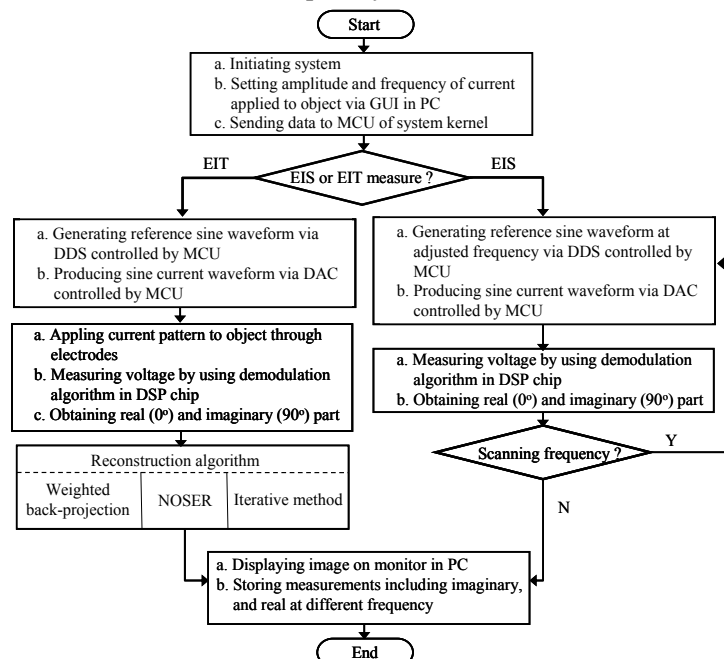
Fig. 2: Flowchart of the system program

3. Preliminary Results and Discussion

3.1. Testing of total harmonic distortion

For the current generator, the total harmonic distortion (THD) at output terminals of DDS or VCCS, for several frequencies such as 1 kHz, 5 kHz, 10 kHz, 50 kHz, 80 kHz, and 100 kHz are measured. The first to sixth harmonic frequencies were used for the calculation. The mean THD at the output terminals of DDS and VCCS is about 0.57% and 0.91%, respectively. These values are equivalent to -45.84 dB and -40.82 dB.

3.2. Linear testing of voltage measurements

The resistance is varied from 0Ω to 1kΩ to test digital demodulation. At different frequencies, the relationships between resistance and measurements of digital raw data are obtained. Because of the limitation of sample rate in the ADC of DSP chip, the sample numbers (N) in one cycle are 100, 50, and 25, at frequency of 1kHz, 10kHz, and 100kHz. We can find good linear characteristic for three fitting lines. The squares of correlation coefficients (R^2) are 0.9994, 0.9988, and 0.9988, respectively. In addition, the load circuit consists of a resistance which is 100Ω, 330Ω, 510Ω and a capacitance which changes from 1nF to 0.47 uF in parallel. At same time, the commercially available LCR instrument with serial number 3532-50 produced by HIOKI Inc. was used to measure the imaginary part (-Xc) of the load circuit. There is also good linearity which square of correlation coefficients are 0.9992 and 0.9878 at frequency of 100k Hz. No matter measure the real or imaginary values, we can obtain good linear relationship.

3.3. Voltage measurements for object

Our simulation tanks were used for experiments to test the current system. Adopting the adjacent excitation strategy, these measured voltages from adjacent electrodes on the boundary. The conductivity of the solution in the tank was 13 mS/cm. The results of the measurements are shown in figure 3.
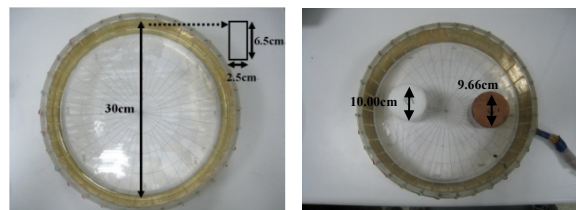

Fig. 3: Simulation tank with 32 electrodes, without targets (left) and within targets (right)

Measurements from adjacent electrodes were utilized to evaluate voltages before using back-projection to reconstruct the images. The electrode slots made of conductive copper and Teflon were separately immersed in a conductive NaCl liquid (1.5 mS/cm) and currents with frequencies of 10 kHz, 60 kHz, and 100 kHz were supplied. Then, impedance values were measured at 0° or 90°, and the cross-sectional image was reconstructed as shown in figure 4. When the separately placed copper target and Teflon target were tested at 60 kHz, the cross sections of the electrical impedance tomography were as shown in figure 5. In addition, the system software was developed using Microsoft Visual C#. At the same time, a graphical user interface was provided for the convenience of the user to extract the electrical impedance data, analyze the data, and reconstruct the image as shown in figure 6.
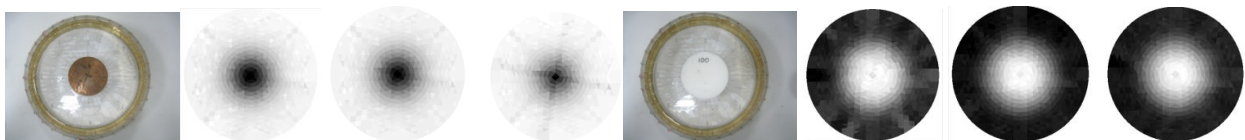
(a) Copper target   10kHz/0^0 60kHz/0^0 100kHz/0^0 (b) Teflon target   10kHz/90^0 60kHz/90^0 100kHz/90^0
Fig. 4: Cross-section of electrical tomography by separately placing (a) conductive copper target (b) Teflon target at different frequencies 0° or 90°.
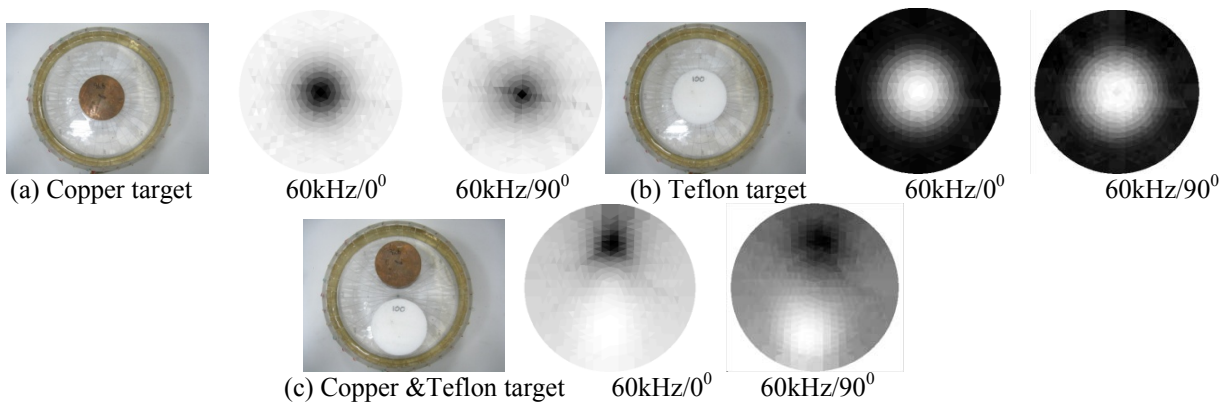
(a) Copper target	60kHz/0^0	60kHz/90^0	(b) Teflon target	60kHz/0^0	60kHz/90^0

(c) Copper &Teflon target   60kHz/0^0 60kHz/90^0

Fig. 5: Electrical impedance tomography taken at 0° and 90° on (a) Copper target (b)Teflon target (c) Copper and Teflon target at 60kHz

4. Conclusions

The system developed can measure both the real and imaginary parts of impedance at any frequency ranging from 100 Hz to 100 kHz. The system uses thirty-two drive/receive electrodes to support two acquisition protocols, which are the adjacent and adaptive methods. The acquisition module is connected to a host PC through a high-speed USB interface. According to the results, the current source based on a direct digital synthesis circuit can produce a current signal with a mean THD of 0.91% at frequencies ranging from 1 kHz to 100 kHz. In the test for a pure resistance ranging from 0 Ω to 1 kΩ at three frequencies, the squares of the correlation coefficients were greater than 0.998. The load circuit included a resistance of 100 Ω, 330 Ω, or 510 Ω, with a capacitance variable from 1 nF to 0.47 μF in parallel. At frequencies of 1 kHz, 10 kHz, and 100 kHz, a highly linear relationship between the measurements and the commercial LCR meter was obtained. Irrespective of the real or imaginary part, the R^2 values were greater than 0.988. Adopting the adjacent excitation strategy, the system was used to measure voltages from adjacent electrodes on the boundary. Therefore, the digital signal processors (DSPs) with high-speed computing capability were utilized as kernels for demodulation. At the same time, the system communicated with a PC via a USB interface and offered its graphical user interface on the PC. Using the DSP demodulator for calculations, the bioelectrical impedance information and EIS characteristics were obtained. In terms of the EIT aspect, back-projection can be used to reconstruct the images. The cross-sectional images of electrical impedance can be obtained for several frequencies at 0° and 90°. The system was tested using two simulation tanks; one is a miniature tank and the other is a normal tank. The system also provides a graphical user interface to extract electrical impedance information, analyze data, and reconstruct images. The impedance values are measured at 0° or 90° and then a cross-sectional image can be reconstructed. When the separately placed copper target and Teflon target were tested, the cross sections of the electrical impedance tomography were obtained. In addition, the system supports the friendly graphic user interface was also provided for the convenience of the user to extract the electrical impedance data, analyze and reconstruct image.
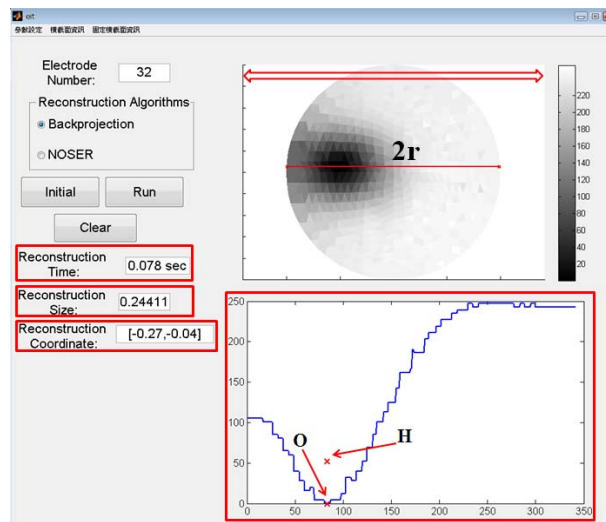

Fig. 6: GUI with the data collection, analysis and reconstruction

5. Acknowledgements

6. References

[1] J. G. Webster, *Electrical Impedance Tomography*, Adam Hilger, IOP, New York, USA, 1990

[2] J. Wilson, P. Milnes, A. R. Waterworth, R. H. Smallwood, and B. H. Brown,"Mk3.5: a modular, multi-frequency successor to the Mk3a EIS/EIT system" *Physiol. Meas.*, Vol. 22, pp. 49-54, 2000

[3] N. Liu, G. J. Saulnier, J. C. Newell, and T. J. Kao, "ACT4: A High-precision, Multi-frequency Electrical Impedance Tomography," *Proc. 6th Conf. on Biomedical Applications of EIT.* London, 2005

[4] A. Keshtkar and R. H. Smallwood, "Electrical impedance spectroscopy and the diagnosis of bladder pathology" *IOP, Physiological Measurement*, vol. 27, pp. 585-596, 2006

[5] K. S. Osterman, T. E. Kerner, D. B. Williams, A. Hartov, S. P. Poplack and K. D. Paulsen, "Multi-frequency electrical impedance imaging: preliminary in vivo experience in breast" *Physiol. Meas.*, vol. 21, pp.99-109, 2000

[6] J. J. Huang, R. J. Wu, "Simulation of the Multi-frequency Current Source for Electrical Impedance Tomography" *Proc. of Annu. Symp. Biomed. Eng. Soc.*, 2007

[+] Ji-Jer Huang. Tel.: +886+6+2533131 ext. 3366; fax: + 886+6+3010073
E-mail address: jjhuang@mail.stut.edu.tw.